

Influence of alkali treatment on physical-mechanical properties of mallow fiber/BOPP composites

Hannah Alagoas Litaiff^{1*} , Gabrielle Machado dos Santos² , Gabriel de Melo³ ,
Claudia da Cunha³  and Virginia Mansanares Giacon¹ 

¹Programa de Pós-graduação em Ciência e Engenharia de Materiais – PPGCEM, Faculdade de Tecnologia – FT, Universidade Federal do Amazonas – UFAM, Manaus, AM, Brasil

²Programa de Pós-graduação em Engenharia e Ciência de Materiais – PPG EnCiMat, Faculdade de Zootecnia e Engenharia de Alimentos – FZEA, Universidade de São Paulo – USP, Pirassununga, SP, Brasil

³Laboratório de Materiais da Amazônia e Compósitos – LaMAC, Faculdade de Tecnologia, Universidade Federal do Amazonas – UFAM, Manaus, AM, Brasil

*hannah.litaiff@ufam.edu.br

Abstract

This study investigated the impact of alkaline treatment on mallow fibers used as reinforcement in bi-axially oriented polypropylene (BOPP) waste composites. Fibers were treated with a 5% NaOH solution and characterized by XRD, FTIR, TGA, and tensile testing. Composites were fabricated with both untreated and treated fibers, and their physical, thermal, morphological, and mechanical properties were evaluated. XRD analysis revealed an increase in crystallinity index after treatment, correlating with enhanced breaking stress in treated fibers. Composites with treated fibers exhibited significantly reduced thickness swelling and water absorption, indicating improved fiber-matrix compatibility. SEM micrographs confirmed enhanced fiber-matrix adhesion in composites using treated fibers. Overall, the results demonstrate that alkali treatment significantly improves the properties of mallow fiber/BOPP composites, promoting their use as sustainable and eco-friendly materials. This research highlights the potential of valorizing agricultural waste and recycled plastics for the development of high-performance composites.

Keywords: *lignocellulosic fiber; mercerization; polymer composite.*

How to cite: Litaiff, H. A., Santos, G. M., Melo, G., Cunha, C., & Giacon, V. M. (2025). Influence of alkali treatment on physical-mechanical properties of mallow fiber/BOPP composites. *Polímeros: Ciência e Tecnologia*, 35(1), e20250006. <https://doi.org/10.1590/0104-1428.20240040>

1. Introduction

Industry sectors, especially civil construction, are increasingly looking for sustainable technological solutions that meet their demands. For that, research has been carried out to develop new materials derived from natural resources, which can be used to add value to these raw materials, as well as guarantee their preservation^[1].

In this context, vegetable fibers are biodegradable materials of renewable origin, found in great abundance and constitute an alternative to synthetic materials, such as fiberglass, widely used since the 1950s^[2]. The advantages of natural fibers are several, including low density, low production cost, high specific strength and modulus of elasticity, in addition to being non-abrasive and non-toxic^[3,4].

Mallow fiber (*Urena lobata L.*) stands out among these diversities because it has great potential and economic viability to be used as a reinforcement material in polymeric composites^[5]. It is cultivated in regions with hot and humid climates, being produced on a large scale in the Amazon region^[6]. It is used as the basis for a variety of manufactured products, the main one being the manufacture of bags for storing food products^[7]. It is widely available, lightweight,

inexpensive, and has superior mechanical properties to other plant fibers such as kenaf fiber^[8].

From another perspective, polypropylene is one of the most versatile thermoplastic polymers and most used in industrial applications^[9]. Bi-axially oriented polypropylene (BOPP) are materials widely used in the flexible packaging sector, mainly for food products, due to their efficiency in physically and chemically preserving packaged products, in line with their low cost and lower environmental impact^[10]. They are recyclable, however, they are not recycled on a large scale, which generates a large amount of waste from this material that has no destination^[11]. One of the ways to reuse this material is to use it in the production of sustainable materials, such as in composite matrix reinforced with vegetable fibers^[12].

However, lignocellulosic fibers are highly hydrophilic due to their chemical components, especially cellulose, which cause poor compatibility with the thermoplastic matrix, which has a polar character, resulting in composites with low resistance to moisture absorption^[13]. On the other hand, there are surface modification methods that minimize these problems and provide better adhesion between fiber and matrix^[14].

To address the challenge of poor adhesion between mallow fibers and PP, a hydrophobic thermoplastic matrix, mercerization can be a suitable option, as it is a well-established treatment for lignocellulosic fibers^[15]. This method reduces the hydrophilicity of the fiber, improving compatibility with the polymer, which increases surface roughness and provides more mechanical anchoring points for stronger fiber-resin bonding^[16]. Through this, it is possible to obtain an improved material with sustainable characteristics and competitive with industrial raw materials, which come from non-renewable sources and cause damage to the environment^[15].

The main objective of this study is to produce polymeric composites with a waste from the manufacturing process of bi-axially oriented polypropylene (BOPP) as matrix and to evaluate the effect of mercerization on the surface of mallow fibers, used as reinforcement material, on their physical, thermal, mechanical and morphological properties.

2. Materials and Methods

2.1. Materials

The mallow fiber used in this study was donated by Companhia Têxtil de Castanhal, located in the municipality of Manacapuru, metropolitan region of Manaus-AM. Waste from the manufacturing process of bi-axially oriented polypropylene (BOPP) films, in the form of flakes and powder, came from the Videolar-Innova S/A factory, located in Manaus-AM. The NaOH used was Anidrol brand.

2.2. Methods

2.2.1. Alkali treatment

Initially, the fibers were cut to a nominal length of 1 cm. The alkaline treatment was carried out according to the methodology adopted by Giacon et al.^[17], which consisted of immersing the mallow fibers in a 5% by weight NaOH solution for 60 min. Subsequently, the fibers were washed with running water until reaching pH 7 and dried at room temperature for 96hrs. The untreated and treated fibers were characterized to investigate the effects of mercerization using the following techniques: XRD, FTIR, TGA and Tensile test.

2.2.2. X-ray diffraction (XRD)

The fibers were analyzed by X-ray diffraction using a Shimadzu diffractometer, model Máxima XDR-7000, operating with copper radiation ($\text{CuK}\alpha$), in which a continuous sweep was performed in the range of $10^\circ < 2\theta < 80^\circ$, at a rate of $2^\circ/\text{min}$ and a step size of 0.02° . The crystallinity index (CI %) was determined according to Segal et al.^[18] using Equation 1:

$$CI\% = \frac{I_{(002)} - I_{(am)}}{I_{(002)}} \times 100 \quad (1)$$

$I_{(002)}$ is related to the crystalline region, corresponding to the maximum diffraction intensity and $I_{(am)}$ is related to the amorphous part, corresponding to the minimum diffraction intensity.

2.2.3. Fourier Transform Infrared Spectroscopy (FTIR)

FTIR spectroscopy was performed on the treated and untreated fibers using a Shimadzu spectrometer (IRAffinity-1s) by horizontal Attenuated Total Reflection (ATR) with diamond prism. Scanning was performed in the infrared region from 4000 to 500 cm^{-1} , with an average of 32 scans for each spectrum.

2.2.4. Thermogravimetric analysis (TGA)

Thermal analysis (TGA/DTG) of samples of about 10 mg of treated and untreated fibers were performed using the SDT Q600 equipment from TA Instrument with a heating rate of $10 \text{ }^\circ\text{C}/\text{min}$ until the final temperature of $700 \text{ }^\circ\text{C}$, with 5.0 nitrogen gas flow of $30 \text{ ml}/\text{min}$ in a 90 microliter alumina crucible without lid.

2.2.5. Tensile test

The single fiber tensile test was performed on treated and untreated fibers with a length of 30 mm according to the ASTM 3379-75^[19] standard in an Oswaldo Filizola universal testing machine, model AME-5KN, with a capacity of 500 Kgf. The specimen model for this test according to ASTM 3379-75^[19] is shown in Figure 1:

To determine the rupture stress, the modulus of elasticity and the deformation, Equations 2, 3 and 4 were used:

$$\sigma = \frac{F}{A} \quad (2)$$

$$E = \frac{\sigma}{\varepsilon} \quad (3)$$

$$\varepsilon = \frac{\Delta l}{l_0} \quad (4)$$

2.2.6. Composite production

Two types of composites were produced, using untreated mallow fibers (UMC) and mallow fibers treated with 5% NaOH (TMC), according to the methodology adopted by Chatterjee et al.^[20], through thermoforming. The proportion

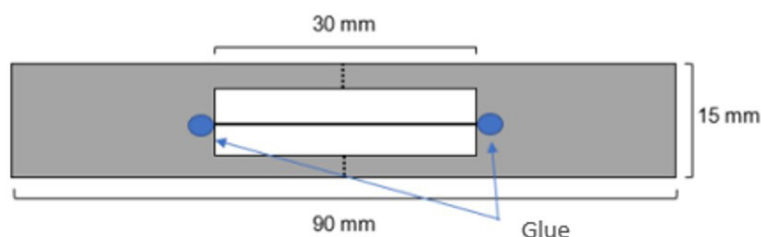


Figure 1. Specimen of single fiber tensile test with ASTM 3379-75 standard.

adopted in the production of composites was 70% by weight of fibers and 30% of BOPP (50% in flakes and 50% in powder). The components were weighed and manually mixed until the fibers were completely enveloped by the BOPP, for approximately 30 min. Afterwards, the mixture was uniformly distributed in a metallic mold with dimensions of $28 \times 28 \times 1$ cm coated with Teflon film and kept in a thermo-hydraulic press at 15 MPa, 170 °C, for 20 min. After pressing, the composites were cooled for 20 min with the aid of a fan and then removed from the mold. Finally, the panels were cut to produce the specimens used in the characterizations. The UMC and TMC composites (Figure 2) were characterized using the following techniques: density, thickness swelling, thermal conductivity, SEM and izod impact test.

2.2.7. Physical properties

The composites were physically characterized according to the Brazilian standard ABNT NBR 15316-2:2019^[21] for the determination of density and thickness swelling for 24 hours and according to the ASTM D570-22^[22] standard to perform the water absorption test. For the density and thickness swelling tests, 10 specimens with dimensions of 50×50 mm were used for each type of composite. For the water absorption test, 5 specimens were used for each type of composite, with dimensions of 76.2×25.4 mm.

2.2.8. Thermal conductivity

The thermal conductivity test was carried out following the specifications of the ASTM D7984-21^[23] standard using a TCi Thermal Conductivity analyzer from the C-Therm brand with thermal capacity from 0 to $50 \text{ W m}^{-1} \text{ K}^{-1}$ and temperature range from -50 to 200 °C. The thermal conductivity was calculated through the average of 10 cycles obtained from 10 samples of 50×50 mm of each type of composite.

2.2.9. Scanning electron microscopy (SEM)

The composites were morphologically characterized through Scanning Electron Microscopy (SEM), using a TESCAN VEGA3 scanning electron microscope. Samples from the internal region and from the surface of the MUC and

MTC composites were fixed with double-sided adhesive tape in aluminum sample holders and metallized with platinum, for 5 min, using the Bal-Tec equipment, model SCD 050. The images were obtained with the microscope operated at a voltage of 15.0 kV.

2.2.10. Izod impact test

The Izod impact test was carried out on the composites according to ASTM D256-10^[24] standard using a Tinius Olsen impact pendulum together with the model 104 controller. 10 specimens of each type of composite were analyzed, with dimensions of 62.5×12.7 mm.

2.2.11. Statistical analysis

The data obtained were treated statistically with analysis of variance (ANOVA), at 5% significance. The null hypothesis (H_0) is the equivalence of the response variables and the alternative hypothesis (H_1) is the non-equivalence; $p\text{-value} > 0.05$ of the test implies accepting H_0 , otherwise it is rejected.

3. Results and Discussions

3.1. X-ray diffraction (XRD)

From the XRD diffractogram (Figure 3) it is possible to notice that the untreated and treated mallow fiber samples present three well-defined main reflection peaks: at $2\theta = 18.7^\circ$, $2\theta = 22.3^\circ$ and $2\theta = 35^\circ$, corresponding to the crystallographic planes (101), (002) and (040), respectively, characteristic planes of type 1 cellulose^[25]. The most intense reflection occurs in the (002) plane for both samples, which corresponds to the lattice planes of the densest glycosidic rings in the structure of cellulose I, being the only naturally occurring polymorphic form of cellulose^[26]. It is also possible to observe that the samples present the same diffraction behavior, with variations only in the intensity of the peaks, thus, it is clear that there was influence of the alkali treatment on the crystallinity of the mallow fiber. The values found for the crystallinity index were 64.64% and 71.28% for untreated and treated mallow

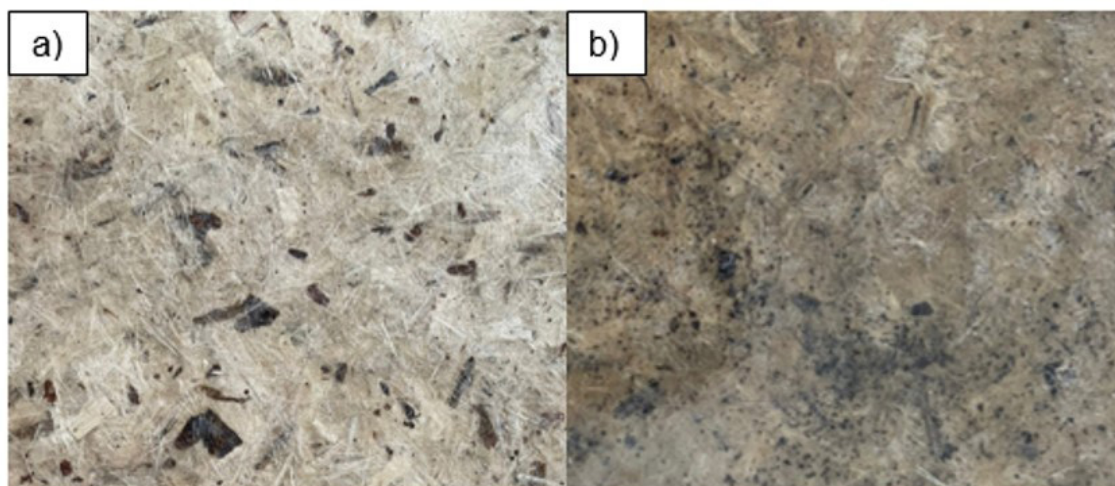


Figure 2. Composite (a) UMC and (b) TMC.

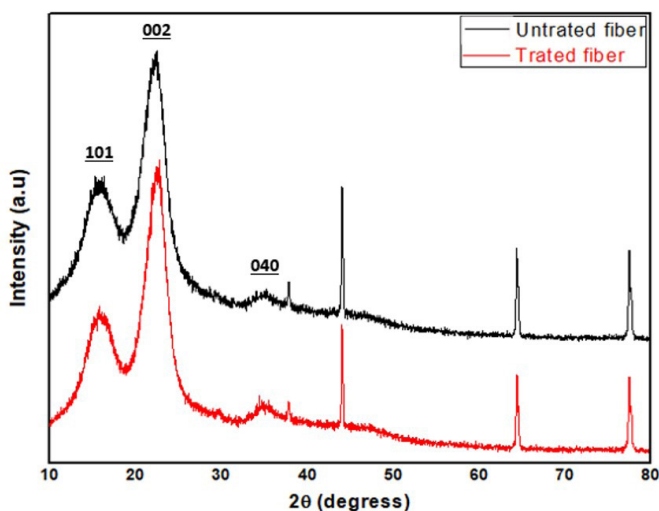


Figure 3. Diffractogram of treated and untreated mallow fibers.

fiber, respectively. This increase indicates that the treatment promoted the reduction of materials such as lignin, hemicellulose and other components that do not confer crystallinity to the fiber. Crystallinity, which is related to the amount of cellulose present in the fiber, increases compared to the untreated fiber due to the formation of hydrogen bonds between the cellulose chains, which results in better packing in the fiber^[27].

3.2. Fourier Transform Infrared Spectroscopy (FTIR)

The FTIR spectra of untreated and treated fibers (Figure 4) show bands characteristic of lignocellulosic fibers. The spectra presents a band at 3400 cm^{-1} , which corresponds to the stretching of hydroxyl groups O-H of cellulose, hemicellulose and lignin^[28]. The transmittance in this peak for the treated fiber spectrum was modified compared with the spectrum of untreated fiber, which is related to the presence of free hydroxyl groups with the breaking of cellulose, hemicellulose and lignin bonds resulting from the mercerization process^[28]. The band at 2897 cm^{-1} is related to the stretching of aliphatic C-H from the methyl $-\text{CH}_3$ and methylene $-\text{CH}_2$ groups, a characteristic functional group of lignocellulosic components present in vegetable fibers^[29]. The band at 1740 cm^{-1} is associated with the C=O stretching of the carbonyl group, present in the acetyl ester or carboxylic groups of hemicellulose, which disappears in the spectrum of the mercerized fiber, indicating high removal of this component and also a change in the chemical composition of the surface fiber after chemical treatment. The band at 1600 cm^{-1} corresponds to the C=C stretching of the aromatic rings, typical of the lignin structure^[30]. There was also a decrease in the band observed at 1242 cm^{-1} , which corresponds to the C-O-C group, present in hemicellulose and lignin, indicating the reduction of these components after chemical treatment^[31]. This same characteristic is found in the bands at 1427 cm^{-1} and 1370 cm^{-1} , associated with vibrations of the C-C bond of aromatic rings and the asymmetric deformation of the methyl group^[7]. The band at 1172 cm^{-1} is associated with stretching of the C-O group of esters and lignin^[7]. The most intense band occurs at 1033 cm^{-1} , which can be associated with the C-H

group and C-O deformations, which are naturally occurring in lignocellulosic fibers^[29]. These results show that the alkali treatment is efficient in removing hemicellulose and lignin fractions from mallow fiber.

3.3. Thermogravimetric analysis (TGA)

From the TGA and DTG curves of untreated and treated fibers (Figure 5) it is possible to observe the existence of four well-defined degradation events. In the first event, there are mass losses of 10.37% and 10.16% in the temperature range of 25-118°C and 25-150°C for untreated and treated fiber, respectively, related to moisture loss due to the evaporation of water^[1]. The second event is related to the process of degradation mainly of hemicellulose, also occurring the beginning of the decomposition of lignin^[32]. For the untreated fiber, the process occurred in the temperature range of 220-310 °C with a mass loss of 14.62%. It is noticed the absence of the characteristic peak of hemicellulose for the treated fiber, indicating that chemical treatment was efficient in its removal^[15]. The third event is due to the decomposition of cellulose, for the untreated fiber there is a mass loss of 51.20% between 309-384 °C and for the treated fiber there is a mass loss of 52.93% between 200-400 °C^[33]. Decomposition of lignin starts at approximately 272 °C for the untreated mallow fiber and at 240 °C for the treated fiber, along with the degradation of the hemicellulose^[32]. Lignin is the most complex lignocellulosic component to degrade, with thermal decomposition over a wide temperature range due to its complex structure, which is overlapped by other peaks^[34]. The fourth event refers to the decomposition of lignin and residual inorganic material^[6]. For the untreated fiber, the degradation occurs in the range of 394-563 °C, with a mass loss of 20.96%, while the treated fiber has a curve longer in this region, starting at approximately 384 °C and extending to a temperature of 674 °C, with a mass loss of 32.30%. At the end of the curves, the ash content, remaining at high temperatures, presented by the untreated and treated fibers of 0.29% and 0.11%, respectively, is observed. In general, the treated fiber is decomposed at

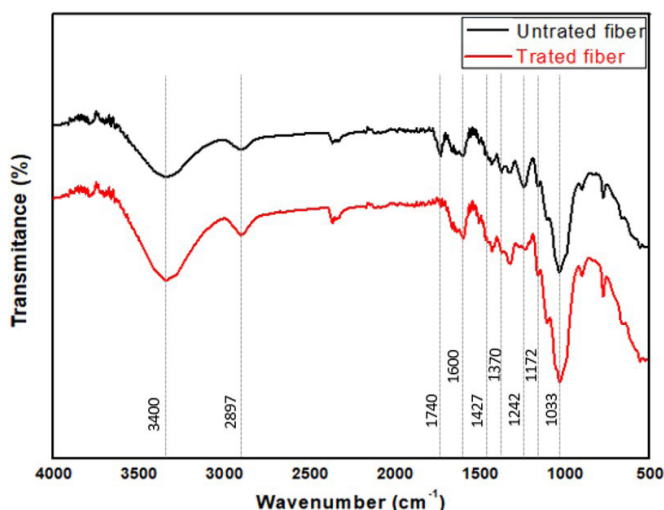


Figure 4. FTIR spectra of treated and untreated mallow fibers.

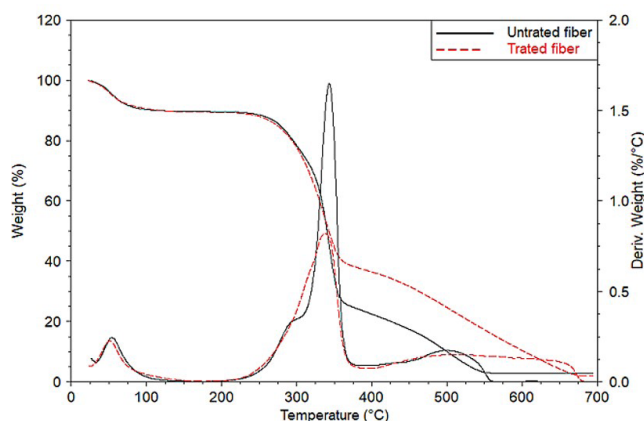


Figure 5. TGA/DTG curves of treated and untreated mallow fiber.

lower temperatures and has greater mass loss compared to the untreated fiber, indicating that the chemical treatment removed the fiber constituents that are thermally unstable, such as hemicelluloses, holocellulose and ash^[35].

3.4. Tensile test

The results of the single-fiber tensile test for tensile strength, modulus of elasticity, elongation at break and the average diameter of treated and untreated mallow fibers are shown in Table 1, which showed a significant difference between them ($p < 0.05$). Also, the table reports the mean values for most common lignocellulosic fibers in raw form, as mentioned in scientific literature^[36].

Compared to the most common lignocellulosic fibers studied in the scientific literature, the already-high mechanical performance of treated mallow fibers stands out, suggesting the potential of mercerization to enhance the mechanical properties of lignocellulosic fibers.

The significant increase in the values obtained for the tensile strength rupture, modulus of elasticity and elongation

at break of the treated fiber in relation to the untreated fiber can be related to the diameter of the fibers^[37]. The average diameters of the fibers decreased with the treatment, from 0.050 mm to 0.042 mm, due to the action of the chemical treatment that acts to remove amorphous materials and cause fibrillation of the fiber bundle, reducing its diameter and increasing its roughness, making them more resistant and rigid^[38]. According to Margem^[7], fibers with smaller diameters have better mechanical tensile properties because they have a greater capacity to absorb energy before fracturing. In addition, the crystallinity index is directly related to the tensile strength and modulus of elasticity of the fiber, that is, the higher the cellulose content present in the fiber, the better its mechanical performance^[39]. Furthermore, the crystallinity index is directly related to the tensile strength and elastic modulus of the fiber^[39]. However, Fonseca^[40] reported that increasing the tensile strength of individual fibers will not necessarily indicate composites with greater mechanical strength. Other characteristics also influence these properties, such as those related to fiber anatomy.

Table 1. Mean values of tensile strength (σ), modulus of elasticity (E), elongation at break (ϵ) and diameter of treated and untreated mallow fibers, as well as other lignocellulosic fibers.

Material	σ (MPa)	E (GPa)	ϵ (%)	Diameter (mm)
Untreated mallow fiber	447.76 \pm 103.03 ^a	59.62 \pm 10.28 ^a	0.76 \pm 0.17 ^a	0.050 \pm 0.008 ^a
Treated mallow fiber	1039.45 \pm 128.15 ^b	88.23 \pm 14.49 ^b	1.20 \pm 0.21 ^b	0.042 \pm 0.006 ^b
Coconut Fiber	100 - 230	2.8 - 6	15 - 38	-
Flax Fiber	345 - 1035	27.6 - 70	1.2 - 3.2	-
Hemp Fiber	270 - 900	23.5 - 90	1.0 - 3.5	-
Jute Fiber	393 - 800	8 - 55	1.0 - 1.8	-
Sisal Fiber	458 - 720	9 - 24	2 - 4.3	-

Table 2. Physical properties of UMC and TMC composites

Composite	Density (Kg/m ³)	D%	Thickness Swelling (%)	Water Absorption (%)
UMC	797.80 \pm 39.42 ^a	7.47	10.59 \pm 4.52 ^a	31.14 \pm 0.45 ^a
TMC	798.43 \pm 16.82 ^a	3.96	4.97 \pm 1.71 ^b	27.41 \pm 0.24 ^b

Mean values with same letter do not present significant statistical variation ($p < 0.05$).

Table 3. Thermal conductivity of UMC and TMC composites.

Composite	Thermal Conductivity (Wm ⁻¹ K ⁻¹)	Effusiveness (Ws ^{1/2} m ⁻² K ⁻¹)	Diffusivity (m ² s ⁻¹ 10 ⁻⁷)
UMC	0.140 \pm 0.048 ^a	313.154 \pm 62.703 ^a	1.923 \pm 0.576 ^a
TMC	0.117 \pm 0.042 ^a	278.144 \pm 70.757 ^a	1.703 \pm 0.373 ^a

Mean values with same letter do not present significant statistical variation ($p < 0.05$).

3.5. Physical properties

Table 2 presents the mean values obtained for the density, density variation (D%), thickness swelling and water absorption of the UMC and TMC composites. With regard to density, the composites do not present a significant difference between them ($p > 0.05$). Both composites showed characteristics of Medium Density Fibreboard (MDF), in accordance with the Brazilian standard ABNT NBR 15316-2:2019^[21], which establishes average density values between 651-800 Kg/m³. The UMC composite showed the highest maximum density variation modulus (D%), corresponding to 7.47%, indicating that the TMC composite has greater stability in relation to this property. For the properties of thickness swelling and water absorption, both composites show a significant difference between them ($p < 0.05$). As for the thickness swelling, both composites showed average values within the limit established by the Brazilian standard ABNT NBR 15316-2:2019^[21] for medium density fiberboard used in dry and wet conditions, which determine maximum values of 17% and 12%, respectively. With regard to water absorption, the minimum requirements are not included in the standard used to carry out the test, however, both composites meet the European Standard EN 317:1993^[41], which establishes a maximum of 35% for this property in fiberboard. For the UMC fiber composite, the higher thickness swelling and water absorption content is associated with the presence of hydroxyl and non-polar groups in various components of the fiber, which are susceptible to water^[42]. Thickness swelling and water absorption in polymeric composites have an intrinsic relationship. In general, the absorption of water causes gradual swelling in the cell walls of the fibers, which expand until saturation. Thus, the micro voids, pores and cracks at the fiber/matrix interface are now occupied by water, increasing the thickness and weight of the composites^[43]. According to Marinho^[44], the higher the residual lignin content in the fiber after chemical treatment,

the lower its vulnerability to water absorption. From this, it is understood that mercerization removed a small part of lignin from the fiber, resulting in a significant improvement in the physical properties of the composites.

3.6. Thermal conductivity

In Table 3, it is possible to compare the results obtained for conductivity, effusivity and diffusivity for the UMC and TMC composites, which did not present a significant difference between them ($p > 0.05$). Fiorelli et al.^[45] characterized particleboard panels of bagasse and sugarcane, curaua and jute fibers and reported results similar to those found in the present study, with an average value of 0.14 W/mK. The alkali treatment tends to increase the thermal conductivity of polymeric composites due to the reduction of voids present at the fiber/matrix interface, increasing the contact area between these components, which facilitates heat transport^[46]. Furthermore, the alkali treatment removes the amorphous components present in the fiber, leading to an increase in crystallinity which in turn improves packing and heat flux in the structure^[47]. Therefore, it was expected that there would be an increase in thermal conductivity for the TMC composite, according to the literature^[46,48], which did not occur in this study. However, both composites showed good thermal conductivity properties and are classified as insulating materials, as they have average values below 0.25 W/mK^[49]. Thus, these materials can be used in applications that require thermal insulation.

3.7. Scanning Electron Microscopy (SEM)

Figure 6 shows the SEM images of the cross section of the UMC and TMC composites, at a scale of 100 μ m. As shown in Figure 6a, it was verified that the UMC composite presented a low adhesion between fiber and matrix, being little homogeneous and having empty spaces due to the lack of wettability with the matrix. The TMC composite

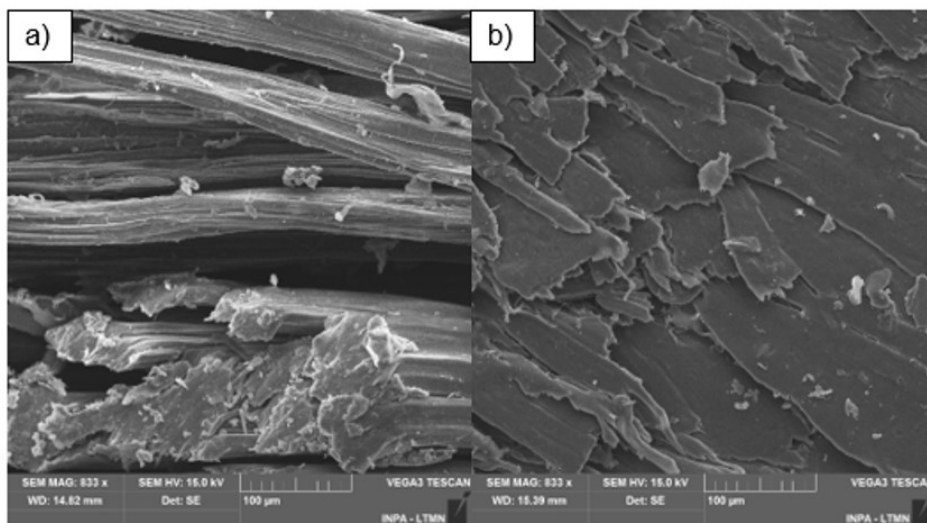


Figure 6. SEM analysis of cross section of (a) UMC and (b) TMC composites

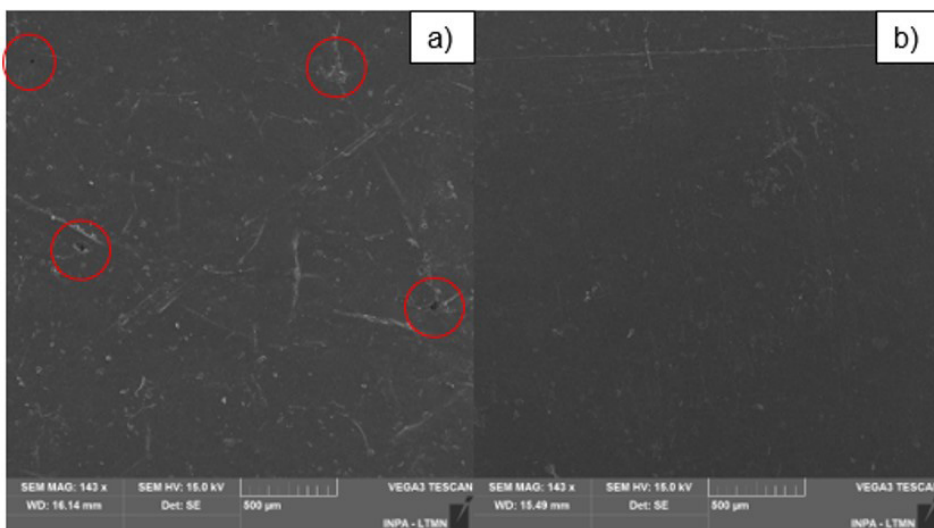


Figure 7. SEM analysis of surface of (a) UMC and (b) TMC composites.

(Figure 6b) presented different characteristics, being homogeneous and uniform, showing that there was good adhesion between fiber/matrix due to the surface treatment. The treatment promoted an increase in the fibrillar surface area, facilitating the anchoring of the fiber to the polymeric matrix and favoring the interfacial adhesion mechanism^[15].

Figure 7 shows SEM images of the surface of UMC and TMC composites. It is possible to observe that the UMC composite (Figure 7a) has pores and cracks throughout its surface, unlike the TMC composite (Figure 7b), which has a smooth surface and no surface defects. These pores and fissures influence the physical properties of the material as they leave the fiber exposed, accumulate water, making the composite heavier and thicker^[43]. These evidenced aspects corroborate the results obtained in the thickness swelling and water absorption tests.

3.8. Izod impact test

Table 4 presents the results obtained in the Izod impact test for the UMC and TMC composites, which did not present a significant difference between them ($p > 0.05$). However, it was expected that the TMC composite would present a higher average value of impact strength when compared to the UMC composite, so that the alkali treatment would make the mallow fiber more resistant to load transfer between fiber/matrix on impact^[50]. As seen in the SEM images, the alkali treatment promoted a better interfacial bond between the fiber and the matrix caused by the removal of amorphous components such as waxes and oils from the fiber surface. According to Senthilkumar et al.^[51], this can lead to a strong mechanical lock between the fiber and the matrix, reducing fiber pullout, which promotes a negative effect on the impact

Table 4. Izod impact strength of UMC and TMC composites.

Composite	Impact strength (J/m)
UMC	293.9 ± 0.3 ^a
TMC	288.2 ± 16.5 ^a

Mean values with same letter do not present significant statistical variation ($p < 0.05$).

strength of the composite. Similar results are found in the literature reported by Senthilkumar et al.^[51] and Goud and Rao^[52], in which an improvement in adhesion between fiber/matrix and a decrease in impact strength was observed with the alkali treatment. Despite this, both composites showed results superior to the impact resistance of other polymeric composites reinforced with other natural fibers, such as PHBV and curaua fiber with impact strength of 169.4 J/m^[53] and recycled PP and royal palm fiber with 35 J/m^[54].

4. Conclusions

The alkali treatment reduced the average diameter of mallow fibers due to the removal of amorphous components from its surface, such as lignin, hemicellulose and organic materials. This led to an increase in the crystallinity index, thermal stability and tensile strength of a single fiber. Thickness swelling and water absorption of the TMC composite were significantly lower compared to the UMC composite. The alkaline treatment did not influence the thermal conductivity of the composites, however, both can be classified as insulating materials. The impact resistance of the composites was not influenced by the chemical treatment. The improvement in the interfacial adhesion mechanism between fiber/matrix with treatment, observed from the SEM images, may have had an impact on this property. Based on this, mallow fibers showed results that demonstrate their potential for use as a source of raw material in polymeric composites, considering that in addition to their satisfactory properties, they promote the reduction of the consumption of non-renewable raw materials, as well as the use of BOPP as a matrix, which adds value to industry waste that has a negative impact on the environment.

5. Author's Contribution

- **Conceptualization** – Virginia Mansanares Giacon; Gabrielle Machado dos Santos.
- **Data curation** – Hannah Alagoas Litaiff.
- **Formal analysis** – Hannah Alagoas Litaiff; Gabriel de Melo.
- **Funding acquisition** – Virginia Mansanares Giacon.
- **Investigation** – Hannah Alagoas Litaiff; Gabrielle Machado dos Santos.
- **Methodology** – Hannah Alagoas Litaiff; Gabrielle Machado dos Santos.
- **Project administration** – Virginia Mansanares Giacon.
- **Resources** – Virginia Mansanares Giacon.
- **Software** – N.A.
- **Supervision** – Virginia Mansanares Giacon.
- **Validation** – Virginia Mansanares Giacon.

- **Visualization** – Hannah Alagoas Litaiff; Gabriel de Melo; Claudia da Cunha.
- **Writing – original draft** – Hannah Alagoas Litaiff.
- **Writing – review & editing** – Gabrielle Machado dos Santos; Gabriel de Melo; Claudia da Cunha; Virginia Mansanares Giacon.

6. Acknowledgements

The authors gratefully acknowledge Companhia Têxtil de Castanhal, Videolar-Innova, Universidade Federal do Amazonas (UFAM) and Laboratório de Materiais da Amazônia e Compósitos (LaMAC). Also, the authors are grateful to the Fundação de Amparo à Pesquisa do Estado do Amazonas (FAPEAM) for financial support. This study was financed in part by the Coordenação de Aperfeiçoamento de Pessoal de Nível Superior – Brasil (CAPES) – Finance Code 001.

7. References

1. Nurazzi, N. M., Asyraf, M. R. M., Rayung, M., Norrahim, M. N. F., Shazleen, S. S., Rani, M. S. A., Shafi, A. R., Aisyah, H. A., Radzi, M. H. M., Sabaruddin, F. A., Ilyas, R. A., Zainudin, E. S., & Abdan, K. (2021). Thermogravimetric analysis properties of cellulosic natural fiber polymer composites: a review on influence of chemical treatments. *Polymers*, 13(16), 2710. <http://doi.org/10.3390/polym13162710>. PMID:34451248.
2. Shaker, K., Nawab, Y., & Jabbar, M. (2020). *Bio-composites: eco-friendly substitute of glass fiber composites*. In O. Kharissova, L. Martínez, & B. Kharisov (Eds.), *Handbook of nanomaterials and nanocomposites for energy and environmental applications* (pp. 1-25). Cham: Springer. http://doi.org/10.1007/978-3-030-11155-7_108-1.
3. Labib, W. A. (2022). Plant-based fibres in cement composites: a conceptual framework. *Journal of Engineered Fibers and Fabrics*, 17, 15589250221078922. <http://doi.org/10.1177/15589250221078922>.
4. Mousavi, S. R., Zamani, M. H., Estaji, S., Tayouri, M. I., Arjmand, M., Jafari, S. H., Nouranian, S., & Khonakdar, H. A. (2022). Mechanical properties of bamboo fiber-reinforced polymer composites: a review of recent case studies. *Journal of Materials Science*, 57(5), 3143-3167. <http://doi.org/10.1007/s10853-021-06854-6>.
5. Costa, U. O., Nascimento, L. F. C., Garcia, J. M., Bezerra, W. B. A., & Monteiro, S. N. (2020). Evaluation of Izod impact and bend properties of epoxy composites reinforced with mallow fibers. *Journal of Materials Research and Technology*, 9(1), 373-382. <http://doi.org/10.1016/j.jmrt.2019.10.066>.
6. Cunha, J. S. C., Oliveira, H. E., No., Giacon, V. M., Manzato, L., & Silva, C. G. (2021). Study on mechanical and thermal properties of amazon fibers on the polymeric biocomposites: malva and Tucum. *Fibers and Polymers*, 22(11), 3203-3211. <http://doi.org/10.1007/s12221-021-0843-y>.
7. Araújo, K. S., & Pereira, H. S. (2017). Public policies and natural fibers: the recent experience of the Amazonian malva and jute production chain. *Amazonian Journal of Agricultural and Environmental Sciences*, 60(1), 60-69. <http://doi.org/10.4322/rca.60102>.
8. Oliveira, P. F., & Marques, M. F. V. (2015). Chemical treatment of natural malva fibers and preparation of green composites with poly (3-hydroxybutyrate). *Chemistry & Chemical Technology*, 9(2), 211-222. <http://doi.org/10.23939/chcht09.02.211>.

9. Liu, W., Cheng, L., & Li, S. (2018). Review of electrical properties for polypropylene based nanocomposite. *Composites Communications*, 10, 221-225. <http://doi.org/10.1016/j.coco.2018.10.007>.
10. Ščetar, M., Kurek, M., Režek Jambrak, A., Debeaufort, F., & Galić, K. (2017). Influence of high power ultrasound on physical-chemical properties of polypropylene films aimed for food packaging: barrier and contact angle features. *Polymer International*, 66(11), 1572-1578. <http://doi.org/10.1002/pi.5415>.
11. Yague, E. T., Mancini, S. D., & Roveda, J. A. F. (2022). Desafios e potenciais soluções para reciclagem de embalagens plásticas flexíveis pós-consumo no Brasil. *Revista DAE*, 70(237), 100-120. <http://doi.org/10.36659/dae.2022.055>.
12. Rohit, K., & Dixit, S. (2016). Mechanical properties of waste biaxially oriented polypropylene metallized films (BOPP), LLDPE: LDPE films with sisal fibres. *American Journal of Engineering and Applied Sciences*, 9(4), 913-920. <http://doi.org/10.3844/ajeassp.2016.913.920>.
13. Lee, C. H., Khalina, A., & Lee, S. H. (2021). Importance of interfacial adhesion condition on characterization of plant-fiber-reinforced polymer composites: a review. *Polymers*, 13(3), 438. <http://doi.org/10.3390/polym13030438>. PMID:33573036.
14. Nunes, J. V. S., Silva, E. X. B., Miranda, M. H. P., Rios, A. S., & Deus, E. P. (2022). Caracterização mecânica e morfológica de fibras de coco tratadas superficialmente para utilização como reforço em polímeros. *Matéria*, 27(2), e20220046. <http://doi.org/10.1590/1517-7076-rmat-2022-0046>.
15. Rebelo, V., da Silva, Y., Ferreira, S., Filho, R. T., & Giacón, V. (2019). Effects of mercerization in the chemical and morphological properties of Amazon Piassava. *Polímeros: Ciência e Tecnologia*, 29(1), e2019013. <http://doi.org/10.1590/0104-1428.01717>.
16. Tavares, F. F. C., Almeida, M. D. C., Silva, J. A. P., Araújo, L. L., Cardozo, N. S. M., & Santana, R. M. C. (2020). Thermal treatment of açai (*Euterpe oleracea*) fiber for composite reinforcement. *Polímeros: Ciência e Tecnologia*, 30(1), e2020003. <http://doi.org/10.1590/0104-1428.09819>.
17. Giacón, V. M., Rebelo, V. S. M., Santos, G. M., Sanches, E. A., Fiorelli, J., Costella, Â. M. S., Melo, G. M. M., & Brito, L. M. A. F. (2021). Influence of mercerization on the physical and mechanical properties of polymeric composites reinforced with Amazonian Fiber. *Fibers and Polymers*, 22(7), 1950-1956. <http://doi.org/10.1007/s12221-021-0460-9>.
18. Segal, L., Creely, J. J., Martin, A. E., Jr., & Conrad, C. M. (1959). An Empirical method for estimating the degree of crystallinity of native cellulose using the X-Ray diffractometer. *Textile Research Journal*, 29(10), 786-794. <http://doi.org/10.1177/004051755902901003>.
19. American Society for Testing and Materials – ASTM. (1975). *ASTM D3379-75: standard test method for tensile strength and young's modulus for high-modulus*. West Conshohocken, PA: ASTM International.
20. Chatterjee, A., Kumar, S., & Singh, H. (2020). Tensile strength and thermal behavior of jute fibre reinforced polypropylene laminate composite. *Composites Communications*, 22, 100483. <http://doi.org/10.1016/j.coco.2020.100483>.
21. Associação Brasileira de Normas Técnicas – ABNT. (2019). *ABNT NBR 15316-2:2019: painéis de fibras de média densidade - parte 2: requisitos e métodos de ensaio*. Rio de Janeiro: ABNT.
22. American Society for Testing and Materials – ASTM. (2022). *ASTM D570-22: standard test method for water absorption of plastics*. West Conshohocken, PA: ASTM International.
23. American Society for Testing and Materials – ASTM. (2021). *ASTM D7984-21: standard test method for measurement of thermal effusivity of fabrics using a Modified Transient Plane Source (MTPS) instrument*. West Conshohocken, PA: ASTM International.
24. American Society for Testing and Materials – ASTM. (2010). *ASTM D256-10: standard test methods for determining the izod pendulum impact resistance of plastics*. West Conshohocken, PA: ASTM International.
25. Tkachenko, T. V., Kamenskyh, D. S., Sheludko, Y. V., & Yevdokymenko, V. O. (2022). Structural and morphological features of microcrystalline cellulose from soybean straw by organosolvent treatment. *Chemistry. Physics and Technology of Surface*, 13(4), 455-466. <http://doi.org/10.15407/hftp13.04.455>.
26. Gabriel, T., Belete, A., Hause, G., Neubert, R. H. H., & Gebremariam, T. (2022). Is mercerization the only factor for (Partial) polymorphic transition of cellulose I to cellulose II in cellulose nanocrystals? *Cellulose Chemistry and Technology*, 56(5-6), 495-507. <http://doi.org/10.35812/CelluloseChemTechnol.2022.56.42>.
27. Shahril, S. M., Ridzuan, M. J. M., Majid, M. A., Bariah, A. M. N., Rahman, M. T. A., & Narayanasamy, P. (2022). Alkali treatment influence on cellulosic fiber from *Furcraea foetida* leaves as potential reinforcement of polymeric composites. *Journal of Materials Research and Technology*, 19, 2567-2583. <http://doi.org/10.1016/j.jmrt.2022.06.002>.
28. Suryanto, H., Sukarni, S., Pradana, Y. R. A., Yanuhar, U., & Witono, K. (2019). Effect of mercerization on properties of mendong (*Fimbristylis globulosa*) fiber. *Songklanakarín Journal of Science and Technology*, 41(3), 624-630. <http://doi.org/10.14456/sjst-psu.2019.73>.
29. Monteiro, S. N., Margem, F. M., Margem, J. I., Martins, L. B. S., Oliveira, C. G., & Oliveira, M. P. (2014). Infra-red spectroscopy analysis of malva fibers. *Materials Science Forum*, 775-776, 255-260. <http://doi.org/10.4028/www.scientific.net/MSF.775-776.255>.
30. Furtado, J. B. M., Furtado, P. A., Fo, Oliveira, T. P., Caetano, M. R. S., Araújo, I. M. S., Figueiredo, F. C., & Santos, J. R., Jr. (2020). Caracterização química da fibra do caule da palmeira de babaçu natural e após tratamento. *Revista de Engenharia e Pesquisa Aplicada*, 5(3), 56-64. <http://doi.org/10.25286/repav5i3.1254>.
31. Fatkhurrohman, Rochardjo, H. S. B., Kusumaatmaja, A., & Yudhanto, F. (2019). *Extraction and effect of vibration duration in ultrasonic process of cellulose nanocrystal (CNC) from ramie fiber*. In *Proceedings of the 1st International Seminar on Advances in Metallurgy and Materials (i-SENAMM 2019)* (pp. 030004). Jakarta: AIP Publishing. <http://doi.org/10.1063/5.0015794>.
32. Asim, M., Paridah, M. T., Chandrasekar, M., Shahroze, R. M., Jawaid, M., Nasir, M., & Siakeng, R. (2020). Thermal stability of natural fibers and their polymer composites. *Iranian Polymer Journal*, 29(7), 625-648. <http://doi.org/10.1007/s13726-020-00824-6>.
33. Xia, L., Zhang, C., Wang, A., Wang, Y., & Xu, W. (2020). Morphologies and properties of *Juncus effusus* fiber after alkali treatment. *Cellulose*, 27(4), 1909-1920. <http://doi.org/10.1007/s10570-019-02933-9>.
34. Ornaghi, H. L., Jr., Ornaghi, F. G., Neves, R. M., Monticeli, F., & Bianchi, O. (2020). Mechanisms involved in thermal degradation of lignocellulosic fibers: a survey based on chemical composition. *Cellulose (London, England)*, 27(9), 4949-4961. <http://doi.org/10.1007/s10570-020-03132-7>.
35. Singh, J. K., & Rout, A. K. (2022). Characterization of raw and alkali-treated cellulosic fibers extracted from *Borassus flabellifer* L. *Biomass Conversion and Biorefinery*, 14(10), 11633-11646. <http://doi.org/10.1007/s13399-022-03238-x>.
36. Laverde, V., Marin, A., Benjumea, J. M., & Ortiz, M. R. (2022). Use of vegetable fibers as reinforcements in cement-matrix composite materials: a review. *Construction & Building Materials*, 340, 127729. <http://doi.org/10.1016/j.conbuildmat.2022.127729>.

37. Silva, F. M. (2018). *Caracterização mecânica de um compósito de matriz poliéster insaturado reforçado com fibras de sisal em diferentes orientações utilizando correlação digital de imagens* (Master's thesis). Universidade Federal Rural do Semiárido, Mossoró.
38. Baskaran, P. G., Kathiresan, M., & Pandiarajan, P. (2022). Effect of alkali-treatment on structural, thermal, tensile properties of dichrostachys cinerea bark fiber and its composites. *Journal of Natural Fibers*, 19(2), 433-449. <http://doi.org/10.1080/15440478.2020.1745123>.
39. Arul Marcel Moshi, A., Ravindran, D., Sundara Bharathi, S. R., Padma, S. R., Indran, S., & Divya, D. (2020). Characterization of natural cellulosic fiber extracted from Grewia damine flowering plant's stem. *International Journal of Biological Macromolecules*, 164, 1246-1255. <http://doi.org/10.1016/j.ijbiomac.2020.07.225>. PMID:32738327.
40. Fonseca, R. P. (2021). *Influência de diferentes tipos de fibras vegetais amazônicas no desempenho de uma argamassa a base de cimento Portland e Metacaulim* (Doctoral dissertation). Universidade Federal de Santa Catarina, Florianópolis.
41. British Standards Institution – BSI. (1993). *EN 317:1993: particleboards and fiberboards: determination of swelling in thickness after immersion in water*. London: BSI.
42. Kamaruddin, Z. H., Jumaidin, R., Ilyas, R. A., Selamat, M. Z., Alamjuri, R. H., & Md Yusof, F. A. (2022). Influence of Alkali treatment on the mechanical, thermal, water absorption, and biodegradation properties of cymbopogon citratus fiber-reinforced, thermoplastic cassava starch–palm wax composites. *Polymers*, 14(14), 2769. <http://doi.org/10.3390/polym14142769>. PMID:35890548.
43. Aparício, R. R. (2019). *Influência das razões de pré-polímero na matriz poliuretânica de óleo de mamona em compósito com alto teor fibras de fibras de piaçava da Amazônia* (Master's thesis). Universidade Federal do Amazonas, Manaus.
44. Marinho, N. P. (2012). *Características das fibras do bambu (Dendrocalamus giganteus) e potencial de aplicação em painéis de fibra de média densidade (MDF)* (Master's thesis). Universidade Tecnológica Federal do Paraná, Curitiba.
45. Fiorelli, J., Galo, R. G., Castro, S. L., Jr., Belini, U. L., Lasso, P. R. O., & Savastano, H., Jr. (2018). Multilayer particleboard produced with agroindustrial waste and Amazonia vegetable fibres. *Waste and Biomass Valorization*, 9(7), 1151-1161. <http://doi.org/10.1007/s12649-017-9889-x>.
46. Sudha, S., & Thilagavathi, G. (2018). Analysis of electrical, thermal and compressive properties of alkali-treated jute fabric reinforced composites. *Journal of Industrial Textiles*, 47(6), 1407-1423. <http://doi.org/10.1177/1528083717695840>.
47. Jena, H., Kumar Pradhan, A., & Kumar Pandit, M. (2017). Effect of cenosphere on thermal conductivity of bamboo fibre reinforced composites. *Advanced Materials & Processes*, 2(2), 97-102. <http://doi.org/10.5185/amp.2017/207>.
48. Scalioni, L. V., Gutiérrez, M. C., & Felisberti, M. I. (2017). Green composites of poly(3-hydroxybutyrate) and curaua fibres: morphology and physical, thermal, and mechanical properties. *Journal of Applied Polymer Science*, 134(14), 44676. <http://doi.org/10.1002/app.44676>.
49. Karwa, R., & Karwa, R. (2020). *One-dimensional steady-state heat conduction*. In: R. Karwa (Ed.), *Heat and mass transfer* (pp. 7-112). Singapore: Springer. http://doi.org/10.1007/978-981-15-3988-6_2.
50. Marichelvam, M. K., Manimaran, P., Verma, A., Sanjay, M. R., Siengchin, S., Kandakodeeswaran, K., & Geetha, M. (2021). A novel palm sheath and sugarcane bagasse fiber based hybrid composites for automotive applications: an experimental approach. *Polymer Composites*, 42(1), 512-521. <http://doi.org/10.1002/pc.25843>.
51. Senthilkumar, K., Rajini, N., Saba, N., Chandrasekar, M., Jawaid, M., & Siengchin, S. (2019). Effect of alkali treatment on mechanical and morphological properties of pineapple leaf fibre/polyester composites. *Journal of Polymers and the Environment*, 27(6), 1191-1201. <http://doi.org/10.1007/s10924-019-01418-x>.
52. Goud, G., & Rao, R. N. (2011). Effect of fibre content and alkali treatment on mechanical properties of Roystonea regia-reinforced epoxy partially biodegradable composites. *Bulletin of Materials Science*, 34(7), 1575-1581. <http://doi.org/10.1007/s12034-011-0361-4>.
53. Beltrami, L. V. R., Scienza, L. C., & Zattera, A. J. (2014). Efeito do tratamento alcalino de fibras de Curauá sobre as propriedades de compósitos de matriz biodegradável. *Polímeros: Ciência e Tecnologia*, 24(3), 388-394. <http://doi.org/10.4322/polimeros.2014.024>.
54. Sá, B. S. R. (2019). *Obtenção e caracterização do compósito de polipropileno reciclado com fibra de palmeira-real (Archontophoenix cunninghamiana)* (Master's thesis). Universidade Tecnológica Federal do Paraná, Londrina.

Received: June 27, 2024

Revised: Sept. 25, 2024

Accepted: Oct. 30, 2024